

Simple hadronic matrix elements with Wilson valence quarks and dynamical staggered fermions at $6/g^2=5.6$

Khalil M. Bitar,^a T. DeGrand,^b R. Edwards,^a Steven Gottlieb,^a U. M. Heller,^a A. D. Kennedy,^a J. B. Kogut,^d A. Krasnitz,^c W. Liu,^e Michael C. Ogilvie,^f R. L. Renken,^g Pietro Rossi,^e D. K. Sinclair,^h R. L. Sugar,ⁱ D. Toussaint,^j and K. C. Wang^k

^aSCRI, Florida State University, Tallahassee, Florida 32306-4052

^bUniversity of Colorado, Boulder, Colorado 80309

^cIndiana University, Bloomington, Indiana 47405

^dUniversity of Illinois, Urbana, Illinois 61801

^eThinking Machines Corporation, Cambridge, Massachusetts 02139

^fWashington University, St. Louis, Missouri 63130

^gUniversity of Central Florida, Orlando, Florida 32816

^hArgonne National Laboratory, Argonne, Illinois 60439

ⁱUniversity of California, Santa Barbara, California 93106

^jUniversity of Arizona, Tucson, Arizona 85721

^kUniversity of New South Wales, Kensington, New South Wales 2203, Australia

(Received 8 January 1993)

We have measured some simple matrix elements for pseudoscalar and vector mesons made of Wilson valence quarks and staggered sea quarks at $\beta=5.6$ at sea quark masses $am_q=0.01$ and 0.025 . Our measurements include the decay constants of pseudoscalars (including f_D), the wave function at the origin (or decay constant) of vector mesons, and the calculation of quark masses from current algebra. The effects of sea quarks on the simulations are small. We make comparisons to quenched simulations at similar values of the lattice spacing ($1/a \simeq 2$ GeV).

PACS number(s): 12.38.Gc, 11.15.Ha, 14.40.-n

I. INTRODUCTION

We have been engaged in an extended program of calculation of the masses and other parameters of the light hadrons in simulations which include the effects of two flavors of light dynamical quarks [1,2]. These quarks are realized on the lattice as staggered fermions. We have carried out simulations with lattice valence quarks in both the staggered and Wilson formulations. In this paper we compute simple matrix elements using valence Wilson quarks. Most previous work with Wilson valence quarks has been done in the quenched approximation. The quenched approximation is uncontrolled, and one would like to know the magnitude of the effects of sea quarks on matrix elements calculated in this approximation. We can do this since we have performed simulations with two masses of sea quarks. We can also compare our results to published results done in the quenched approximation at equivalent values of the lattice spacing. Including the effects of staggered sea quarks is computationally less intense than using Wilson sea quarks, and we consider that mixing the two realizations is not inappropriate for a first round of numerical simulations.

We have measured matrix elements of the form $\langle h|A_\mu|0\rangle$ and $\langle h|V_\mu|0\rangle$, where A_μ is an axial-vector current and V_μ is a vector current. Physically, these quantities parametrize the decay constants of pseudoscalar and vector mesons. Valence quark masses range from very light through the charmed quark mass. In particular, we will present a prediction for the decay constant of

pseudoscalars containing a charmed quark. As a by-product of the axial-vector current measurement, we measure a quantity which is proportional to the valence quark mass m_q . In addition, we determine the renormalization factors (or ratios of renormalization factors) from various definitions of vector and axial-vector currents, which can then be compared to perturbation theory and to other simulations.

The lattices we use are the ones we generated in our most recent round of simulations [2] on $16^3 \times 32$ lattices at a lattice coupling of $\beta=5.6$. The simulations include two flavors of dynamical staggered fermions; the dynamical fermion masses are $am_q=0.01$ and $am_q=0.025$.

We should warn the reader that these simulations are performed at values of the lattice spacing which are quite a bit greater than those used by present-day quenched simulations. Depending on the particle whose mass is used to set the lattice spacing, our lattice spacing a lies in the range $1/a=1700-2100$ MeV. Thus we expect considerable contamination from lattice artifacts. Probably the most reasonable quenched approximation data sets with which to compare to are ones taken at $\beta \leq 6.0$, since they are thought to have a similar lattice spacing. (For example, the APE collaboration [3] has determined a lattice spacing from quenched Wilson spectroscopy of $1/a=2132$ MeV, by extrapolating the ρ mass to zero valence quark mass or to the critical hopping parameter κ_c .) At the parameter values of these simulations, spectroscopy is essentially identical to that from quenched simulations.

We would now like to summarize our main results, saving technical details for the main body of the paper. We are primarily interested in seeing whether sea quarks affect simple matrix elements. We do this by comparing to results from quenched simulations at values of the lattice spacing close to ones we use, as well as to experimental data. These comparisons are best done when the matrix element is expressed in physical units (GeV) as a function of physical units (particle masses or mass ratios). However, converting a lattice number to a continuum number is not straightforward. In addition to a multiplication by some power of the lattice spacing (to set the dimension), lattice operators generally require a renormalization to convert from lattice to continuum regularization. We do this in two ways, using a “conventional” perturbation theory and a “tadpole-improved” method recently proposed by Lepage and Mackenzie [4]. We first consider the wave function at the origin of vector mesons, parametrized by

$$\langle V | V_\mu | 0 \rangle = \frac{1}{f_V} m_V^2 \epsilon_\mu. \quad (1.1)$$

We present our calculation of f_V using the lattice conserved (Wilson) vector current in Fig. 1. We see that the results show little dependence on the sea quark mass. In Fig. 2 we compare the conserved current to results from another lattice definition of the current, using the “conventional” lattice-to-continuum renormalization. We compare our results to those from quenched simulations using the same definition and renormalization prescription. We see that our results are quite similar to the quenched ones. Variation in our results due to different sea quark masses is small compared to the variation in the predicted continuum result due to different lattice-to-continuum conversions.

The second observable is the decay constant f_P of a pseudoscalar meson containing one light quark and one heavy quark (such as the D or B meson). It has become

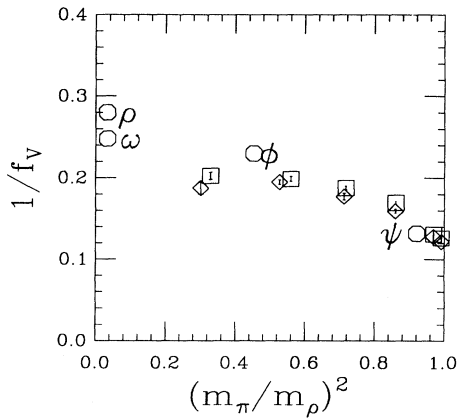


FIG. 1. Lattice $1/f_V$ from the conserved (Wilson) vector current, as a function of $(m_\pi/m_\rho)^2$, using tadpole-improved perturbation theory. The labeled points are physical particles. Results from simulations with sea quark mass $am_q=0.01$ are shown as squares and for sea quark mass $am_q=0.025$ as diamonds.

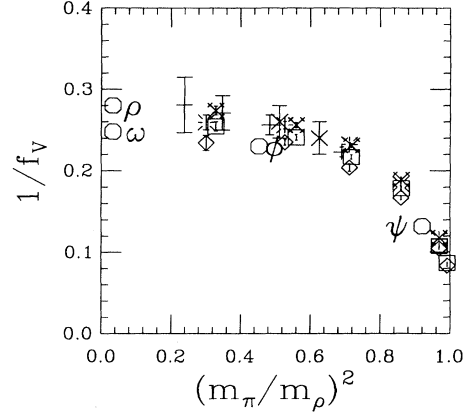


FIG. 2. Lattice $1/f_V$ as a function of $(m_\pi/m_\rho)^2$, using conventional field normalization and perturbative corrections. The labeled points are physical particles. Results for the conserved (Wilson) vector current from simulations with sea quark mass $am_q=0.01$ are shown as squares and for sea quark mass $am_q=0.025$ as diamonds. Results for the local vector current, scaled by a phenomenological $Z_V=0.57$ from simulations with sea quark mass $am_q=0.01$, are shown as fancy crosses and for sea quark mass $am_q=0.025$ as bursts. Quenched $\beta=6.0$ from Daniels *et al.* [19] are crosses and APE results [3] are pluses.

conventional to display $f_P \sqrt{M_P}$ as a function of the inverse pseudoscalar mass $1/M_P$, since it is expected that f_P scales as $1/\sqrt{M_P}$ for large M_P . We measured two lattice operators corresponding to the continuum axial-vector current and performed the lattice-to-continuum transcription using both “conventional” and “tadpole-improved” prescriptions. We show our results for each of those prescriptions in Figs. 3 and 4. Here the lattice

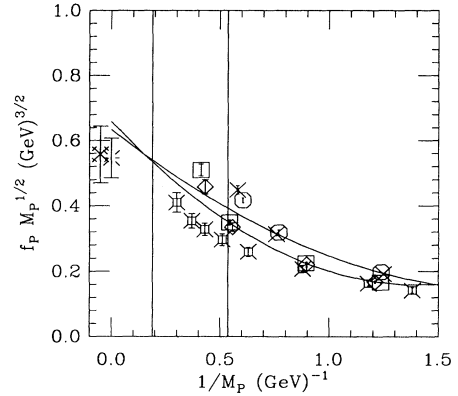


FIG. 3. Quantity $f_P \sqrt{M_P}$ as a function of the inverse pseudoscalar mass, with lattice data analyzed using tadpole-improved perturbation theory. Data for static quarks are from Ref. [26] (fancy cross); burst is Ref. [27]. The fancy squares are the data of Bernard *et al.* [5], analyzed using “exp(ma)” field normalization. The scale is set by f_π . Our data are local and nonlocal currents at sea quark mass 0.025 (diamonds and octagons) and local and nonlocal currents at sea quark mass 0.01 (squares and crosses). The curves are the quadratic fits described in the text. The vertical lines identify the points corresponding to f_B and f_D .

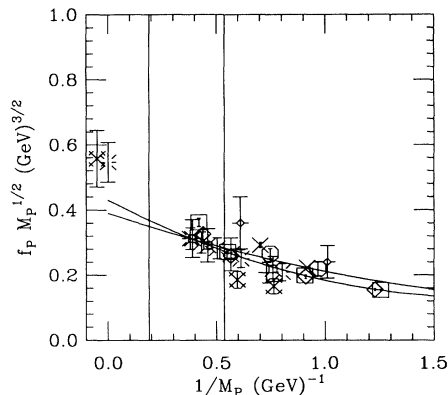


FIG. 4. Quantity $f_p \sqrt{M_p}$ as a function of the inverse pseudoscalar mass, with lattice data analyzed using conventional field normalization. Data for static quarks are from Ref. [26] (fancy cross); squares are Ref. [27]. Other dynamic heavy quark data are from the European Lattice Collaboration [23] (fancy squares), Gavela *et al.* [22] (plus signs), and DeGrand and Loft [24] (fancy diamonds). The scale is set by f_π . Our data are local and nonlocal currents at sea quark mass 0.025 (diamonds and octagons) and local and nonlocal currents at sea quark mass 0.01 (squares and crosses). The curves are the quadratic fits described in the text. The vertical lines identify the points corresponding to f_B and f_D .

spacing has been chosen by fitting f_π to its real-world value 132 MeV. Again, our results show little variation with respect to sea quark mass. The predictions using “conventional” renormalization are quite similar to quenched results, while the “tadpole-improved” predictions are quite a bit higher than both the “conventional” normalization results and the quenched results of Bernard *et al.* [5], from simulations performed at smaller lattice spacing. Our message for the reader is that our results show little variation with sea quark mass and resemble quenched results from simulations performed at a similar value of the lattice spacing, while at this value of the lattice spacing our results depend rather more strongly on the prescription for converting lattice results to continuum results than they do on sea quark properties.

The outline of the rest of the paper is as follows. In Sec. II we describe the lattice simulations and the data set. In Sec. III we describe the methodology for extracting matrix elements from the data. In Sec. IV we describe the program for converting lattice numbers to continuum numbers and compare some results to perturbation theory. Sections V, VI, and VII describe the vector decay constant, quark masses, and the pseudoscalar decay constant. A few conclusions are in Sec. VIII.

II. THE SIMULATIONS

A. Numerics

Our simulations were performed on the connection machine CM-2 located at the Supercomputer Computa-

tions Research Institute at Florida State University.

We carried out simulations with two flavors of dynamical staggered quarks using the hybrid molecular dynamics (HMD) algorithm [6]. The lattice size is $16^3 \times 32$ sites and the lattice coupling $\beta=5.6$. The dynamical quark mass is $am_q=0.01$ and 0.025. The total simulation length was 2000 simulation time units (with the normalization of Ref. [1]) at each quark mass value. We recorded lattices for the reconstruction of spectroscopy every 20 HMD time units, for a total of 100 lattices at each mass value.

We computed spectroscopy with staggered sea quarks at six values of the Wilson quark hopping parameter: $\kappa=0.1600, 0.1585, 0.1565, 0.1525, 0.1410$, and 0.1320. The first three values are rather light quarks (the pseudoscalar mass in lattice units ranges from about 0.25 to 0.45), and the other three values correspond to heavy quarks (pseudoscalar masses of from 0.65 to 1.5). We computed properties of mesons with all possible combinations of quark and antiquark mass; this will allow us to study matrix elements of strange and charm mesons. We used periodic boundary conditions in all four directions of the lattice. We fix gauge in each configuration in the data set to lattice Coulomb gauge using an overrelaxation algorithm [7]. Our inversion technique is conjugate gradient with preconditioning via incomplete lower-upper (ILU) decomposition by checkerboards [8]. We used a fast matrix inverter written in CMIS (connection machine instruction set) [9].

B. Interpolating fields

Matrix elements are determined from correlation functions such as

$$C_{ij}(\mathbf{k}=0, t) = \sum_{\mathbf{x}} \langle O_i(\mathbf{x}, t) O_j(\mathbf{0}, t=0) \rangle. \quad (2.1)$$

Just as in the case of spectroscopy, a good interpolating field is necessary so that the correlator is dominated by the lightest state in its channel at small times separation. We have chosen to use an interpolating field which is separable in the quark coordinates and extended in the coordinates of either quark:

$$O_1(\mathbf{x}, t) = \sum_{y_1, y_2} \phi_1(\mathbf{y}_1 - \mathbf{x}) \phi_2(\mathbf{y}_2 - \mathbf{x}) c_q(\mathbf{y}_1, t)^\dagger \Gamma c_{\bar{q}}(\mathbf{y}_2, t)^\dagger. \quad (2.2)$$

Here $c_i(\mathbf{y}, t)^\dagger$ are creation operators for the quark and antiquark, Γ is the appropriate Dirac matrix, and we have suppressed all color and spin indices. Since the operator is separable, the individual ϕ terms are sources for calculation of quark propagators. We take $\phi(\mathbf{x})$ to be a Gaussian centered around the origin:

$$\phi(\mathbf{x}) = \exp[-(|\mathbf{x}|/r_0)^2]. \quad (2.3)$$

The parameter r_0 can be chosen to give an optimal overlap with the ground state.

We need zero-spatial-momentum correlation functions with O_1 also as the sink:

$$\begin{aligned}
C_{11}(\mathbf{k}=0, t) &= \sum_{\mathbf{x}} \langle O_1(\mathbf{x}, t) O_1(0, 0) \rangle \\
&= \sum_{\mathbf{x}} \left\langle \sum_{y_1, y_2} \phi_1(y_1 - \mathbf{x}) \phi_2(y_2 - \mathbf{x}) \Gamma^\dagger G_q(y_1, t; \phi_1, t=0) \Gamma G_{\bar{q}}(y_2, t; \phi_2, t=0) \right\rangle.
\end{aligned} \tag{2.4}$$

Here

$$G_i(\mathbf{y}, t; \phi, t=0) = \sum_{\mathbf{z}} G_i(\mathbf{y}, t; \mathbf{z}, t=0) \phi(\mathbf{z})$$

is obtained as the inverse of the fermion matrix on a source $\phi(\mathbf{z})$ on the time slice $t=0$. Going to Fourier transforms, we can write this as

$$C_{11}(\mathbf{k}=0, t) = \sum_{\mathbf{p}} \langle \tilde{\phi}_1(\mathbf{p}) \tilde{\phi}_2(-\mathbf{p}) \Gamma^\dagger \tilde{G}_q(-\mathbf{p}, t; \phi_1, t=0) \Gamma \tilde{G}_{\bar{q}}(\mathbf{p}, t; \phi_2, t=0) \rangle, \tag{2.5}$$

requiring, as for local sinks, only one sum over a time slice, plus the cost of taking the Fourier transforms \tilde{G}_i and $\tilde{\phi}_j$. The latter can be precomputed once for the whole simulation. Using fast Fourier transforms (FFT's) this computation becomes practical. For our six κ values combined, it took only about 25% longer than a computation using point or wall sources and sinks.

We performed a small test to determine reasonable r_0 's: We took 24 lattices and calculated hadronic spectroscopy at two hopping parameter values $\kappa=0.1410$ and 0.1585 , at sea quark mass 0.025 , and three values of r_0 at each κ . We show effective-mass plots for hadrons made of degenerate heavy quarks and degenerate light quarks in Figs. 5 and 6. While the light quark spectroscopy was not very sensitive to r_0 , the heavy quark spectroscopy was: A larger r_0 was optimal. Following these tests, we chose the following r_0 values for each κ [shown as (κ, r_0)]: $(0.1320, 2.5)$, $(0.1410, 3.0)$, $(0.1525, 3.5)$, $(0.1565, 4.0)$, $(0.1585, 4.5)$, and $(0.1600, 5.0)$. On the full data set we checked all the hadronic spectroscopy and found agree-

ment between results using these sources with our earlier work using a "wall" (uniform) source.

III. GENERAL FORMALISM FOR LATTICE MATRIX ELEMENTS

All measurements of matrix elements involve determining ratios of correlation functions. We have two generic classes of correlators: ones in which the two operators are different (one of the operators is to be determined and the other is not) [C_{12} of Eq. (2.1)] and a class where both operators are identical to one of the operators in the preceding equation [$C_{11}(t)$]. For example, O_1 could be a Gaussian interpolating field and O_2 could be a current.

Passing to momentum space and inserting a complete set of relativistically normalized states, we have

$$C_{ij}(t) = \sum_n \frac{1}{2\mu_n} \langle 0 | O_i | n(k=0) \rangle \langle n(k=0) | O_j | 0 \rangle e^{-\mu_n t}. \tag{3.1}$$

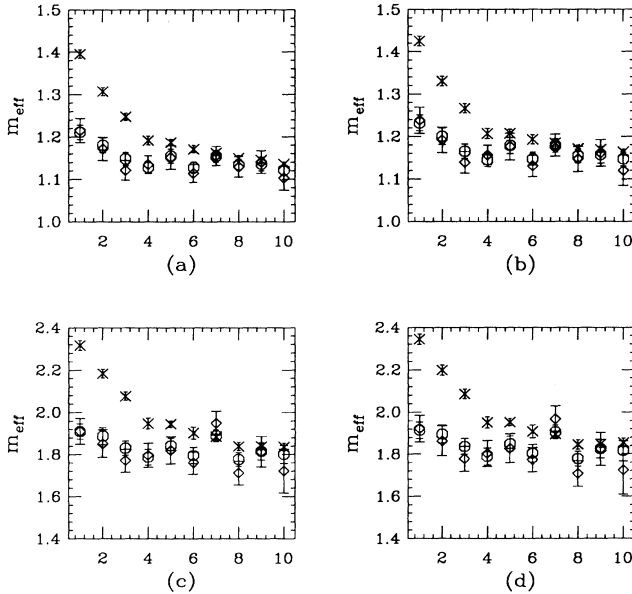


FIG. 5. Effective masses for $\kappa=0.1410$ as a function of r_0 : $r_0=1$ (crosses), $r_0=2.5$ (octagons), and $r_0=4.0$ (diamonds). Figures are (a) pion, (b) ρ , (c) nucleon, and (d) Δ .

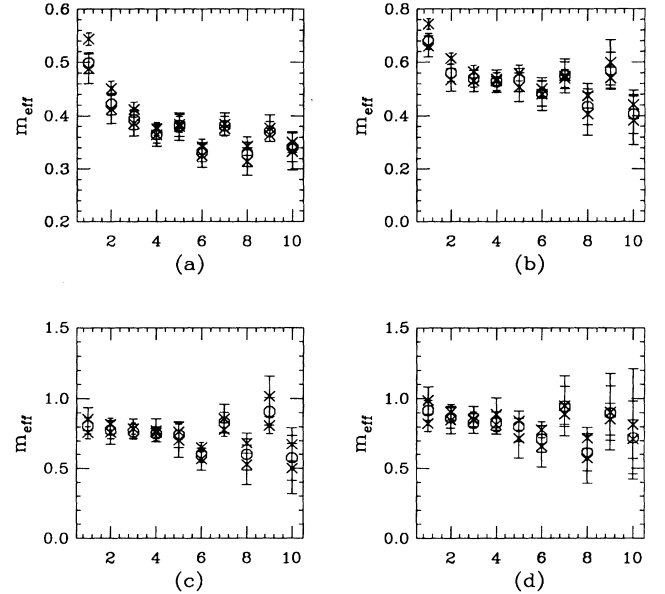


FIG. 6. Effective masses for $\kappa=0.1585$ as a function of r_0 : $r_0=3.0$ (crosses), $r_0=4.0$ (octagons), and $r_0=5.0$ (diamonds). Figures are (a) pion, (b) ρ , (c) nucleon, and (d) Δ .

At large t only one state (of mass μ) should dominate the sum, and we expect to see

$$C_{12}(t) = \frac{1}{2\mu} e^{-\mu t} \langle 0 | O_1 | h \rangle \langle h | O_2 | 0 \rangle \quad (3.2)$$

and

$$C_{11}(t) = \frac{1}{2\mu} e^{-\mu t} \langle 0 | O_1 | h \rangle \langle h | O_1 | 0 \rangle. \quad (3.3)$$

Of course, it is incorrect to compute $\langle h | O_2 | 0 \rangle$ by directly taking ratios of C_{12} to C_{11} . The correct way to analyze the data, which produces a meaningful χ^2 , is to do a three-parameter $(\mu, \langle 0 | O_1 | h \rangle, \langle h | O_2 | 0 \rangle)$ simultaneous fit to both data sets which includes the full correlation matrix. This is how we analyze all our data. This fitting method also allows us to quote a meaningful confidence level for a fit. Reference [10] discusses this fitting procedure in detail. A typical set of correlators and their fits are shown in Fig. 7.

One feature shown by all the operators we studied was the very poor confidence level of fits to operators containing one (or two) heavy quarks, especially the $\kappa=0.1320$ quark. We saw this same behavior in our spectroscopy in Ref. [2]. The culprit is the correlator with a local current at one end. While the extended operator has reasonable overlap on the ground state, the local current does not. In other words, $J(x,t)|0\rangle$ creates excited-state mesons much more readily than it creates ground states. Thus we do not see a plateau in the effective mass of the state. The operator itself drifts with fitting range, too. The same problem has crippled other calculations of heavy-light matrix elements [11]. An example of this behavior is shown for the local axial-vector current matrix element, in Fig. 8.

Since we have so many different operators and quark masses, it is necessary to give some general rule for selecting the best-fit value to present in a figure or table. In selecting the distance range to be used in the fitting, we have tried to be systematic. We somewhat arbitrarily

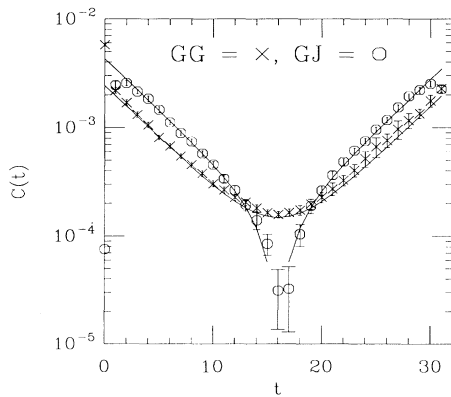


FIG. 7. Data and results of a three-parameter correlated fit to Gaussian source and sink (crosses) and to a Gaussian source and local axial-vector current sink ($\bar{\psi}\gamma_5\psi$) (octagons) for $am_q=0.01$ sea quark mass and $\kappa=0.1600$ valence quarks. The second correlator is antiperiodic, and its absolute value is shown.

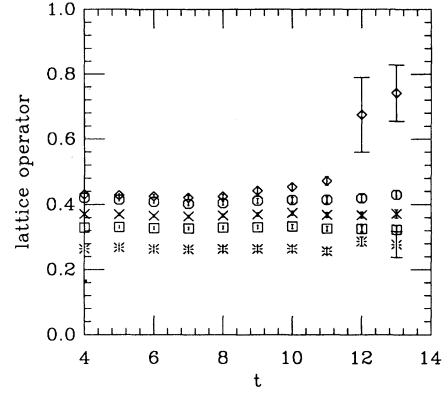


FIG. 8. Results of fits to the lattice matrix element $\langle 0 | \bar{\psi}\gamma_5\psi | P \rangle$ over the range t to $t_{\max}=15$, from three parameters fits to two propagators. The diamond, octagon, cross, and square are for heavy-quark-light-quark pseudoscalars with heavy $\kappa=0.1320, 0.1410, 0.1525$, and 0.1565 , and the burst is for a meson made of two light quarks. In all cases the light quark hopping parameter is $\kappa=0.1600$.

choose the best fitting range as the range which maximizes the confidence level of the fit (to emphasize good fits) times the number of degrees of freedom (to emphasize fits over big distance ranges) divided by the statistical error on the mass (to emphasize fits with small errors). We typically restrict this selection to fits beginning no more than 11 or 12 time slices from the origin. This was the method we used to select the best mass in our earlier work [1].

When we have to extrapolate a quantity (for example, to zero quark mass), we combine correlated fits with jack-knife averages. We perform a series of fits where ten successive lattices are removed from the data set, select the best-fit value of the matrix element using the procedure described in the last paragraph, extrapolate the desired quantity for the subset of data, and then perform a jack-knife average of the extrapolated quantity.

IV. FROM LATTICE TO CONTINUUM NUMBERS

Next we must discuss how we convert lattice measurements into predictions of continuum observables. There are three complications: First, dimensionful observables require a lattice spacing to set the scale. Since the simulations do not show proper mass ratios for hadrons at better than the fifteen percent level, we cannot claim to know the lattice spacing better than this. Second, lattice operators require perturbative renormalizations to convert them to continuum ones. Third, there are additional corrections [$O(a)$ corrections] which arise because the lattice operators themselves differ from the continuum operators by terms proportional to the lattice spacing a . Thus the continuum matrix element is related to the lattice one by

$$\langle f | O^{\text{cont}}(\mu) | i \rangle = a^D [Z(\mu a, g(a)) \langle f | O^{\text{latt}}(a) \rangle + O(a) + O(g^2 a) + \dots] \quad (4.1)$$

(D is the engineering dimension of the matrix element.)

A symptom of the presence of $O(a)$ contributions is an apparent dependence of the Z parameter on initial and final states. These corrections can be ameliorated by using “improved operators” [12,13]. This study used only unimproved operators, however, and the $O(a)$ corrections remain an unknown systematic.

The Z factors are a product of two terms. The first is a lattice to continuum regularization conversion factor which in perturbation theory is a power series in α_s . The second term is an overall multiplication by a function of the hopping parameter κ which relates the field normalization for Wilson fermions to the continuum fermion normalization.

There are two ways to assign this normalization. The first is to relate the action of Wilson fermions to the continuum action. This gives a multiplication factor of $\sqrt{2\kappa}$ as the conversion between Wilson and continuum fermions.

The second way follows a recent paper by Lepage and Mackenzie [4]. They suggest a program for calculation of renormalization terms which has two parts: “tadpole-improved” perturbation theory and a choice of a subtraction scheme for perturbative calculations which attempts to minimize higher-order corrections.

Tadpole-improved perturbation theory for Wilson fermions is based on the observation that ordinary perturbation theory, based on the naive expansion

$$U_\mu(x) = 1 + ig_a A_\mu(x) + \dots, \quad (4.2)$$

is a misleading expansion in g . Higher-order terms in the expansion of the exponential contain higher powers of agA_μ and the ultraviolet divergences from contractions of A 's cancel the extra a 's, leaving these terms suppressed not by powers of ga , but only by powers of g . These contributions are the QCD tadpole corrections. Tadpoles renormalize the link operator (at least in smooth gauges), and so Lepage and Mackenzie suggest writing

$$U_\mu(x) = u_0 [1 + ig_a A_\mu(x) + \dots], \quad (4.3)$$

where u_0 is chosen nonperturbatively. This suggests replacing U_μ in the action by the combination U_μ/u_0 , so that the tadpole-improved action for Wilson fermions is

$$S = \sum_n \bar{\psi}_n \psi_n - \tilde{\kappa} \sum_{n\mu} \left[\bar{\psi}_n (1 - \gamma_\mu) \frac{U_\mu(n)}{u_0} \psi(n + \mu) \right] + \dots \quad (4.4)$$

Here $\tilde{\kappa} = \kappa u_0$. At the tree level $\tilde{\kappa} = \frac{1}{8}$ and one might expect that $\kappa_c \simeq 1/8u_0$.

Now compute the field renormalization in the following way: Compute the quark two-point functions $S_F(ip_0, \mathbf{p}=0)$. Near its pole

$$S_F(ip_0) \simeq \frac{1 + \gamma_0}{2} \frac{1}{p_0 - \mu} \frac{1}{1 - 6\tilde{\kappa}}, \quad (4.5)$$

where the quark mass μ solves $1 - 6\tilde{\kappa} = 2\tilde{\kappa} \exp(-\mu)$. [This is the “exp(ma) factor” recently advocated by Bernard, Labrenz, and Soni [5] in their analysis of pseudo-scalar decay constants.] This implies that $\psi_{\text{cont}} = \sqrt{1 - 6\tilde{\kappa}} \psi_{\text{latt}}$ or that the overall field renormaliza-

tion factor should be $\sqrt{1 - 3\kappa/4\kappa_c}$.

This is different from the conventional $\sqrt{2\kappa}$ field renormalization. For our data, where at sea quark mass $am = 0.01$, $\kappa_c = 0.1610$, the square of the field renormalization in this prescription varies from 0.385 to 0.255 as κ varies from 0.1320 to 0.1600, while the variation in the naive prescription is only 21%, and the factors vary from 0.262 to 0.32.

To calculate tadpole-improved renormalizations of matrix elements for massless quarks, Lepage and Mackenzie give the following prescription: For local operators, replace the $\sqrt{2\kappa_c}$ field renormalization by the perturbative expansion for κ_c [14],

$$2\kappa_c = \frac{1}{4}(1 + 1.364\alpha_s), \quad (4.6)$$

so that a bilinear $\bar{\psi}\Gamma\psi$, with a perturbative Z factor of $(1 + A\alpha_s)2\kappa_c$, becomes $\frac{1}{4}[1 + (A + 1.364)\alpha_s]$ or at $\kappa \neq \kappa_c$ $[1 + (A + 1.364)\alpha_s](1 - 3\kappa/4\kappa_c)$. This lowers the coefficient of α_s if A is negative (which it is for all bilinears we have seen). Operators already containing a link ($\bar{\psi}\Gamma U\psi$) automatically include the u_0 factor and the only change they require is to convert $2\kappa_c$ into $\frac{1}{4}$. Table I shows the renormalization factors for all the operators used in this study. They are given in Refs. [4,14,15].

Lepage and Mackenzie suggest picking $u_0 = \langle \frac{1}{3} \text{Tr} U_P \rangle^{1/4}$ as a nonperturbative definition of u_0 in terms of the measured plaquette. In our simulations we found $\langle \frac{1}{3} \text{Tr} U_P \rangle = 0.56500(2)$ and $0.56444(2)$ at $am_q = 0.01$ and 0.025 (note the tiny dependence on the quark mass). This would give $\kappa_c = 1/8u_0 = 0.1442$ for both $am_q = 0.01$ and 0.025 , to be compared with 0.1610 and 0.1613 , respectively. The tadpole gives about half the observed renormalization in κ_c .

We will present results from both normalization schemes since most published calculations of matrix elements use the conventional normalization. This will also give the reader a feel for the magnitude of systematics in lattice calculations which are not due to the simulations themselves.

Next one must define the coupling α_s . Lepage and Mackenzie argue that the lattice coupling $\alpha_{\text{latt}} = 6/4\pi\beta$ is a poor expansion parameter since with it coefficients of second-order corrections are large. They suggest using an alternative coupling defined through the plaquette [16]

$$-\ln \langle \frac{1}{3} \text{Tr} U_P \rangle = 4.18879\alpha_V(3.41/a) \times \{1 - (1.185 + 0.070n_f)\alpha_V + O(\alpha_V^2)\}. \quad (4.7)$$

TABLE I. Tadpole-improved renormalization factors for operators used in this study.

Operator	Name	Z factor
$\bar{\psi}\gamma_5\psi$	Z_P	$\frac{1}{4}(1 - 1.03\alpha_V)$
$\bar{\psi}\gamma_5\gamma_\mu\psi$	Z_A^I	$\frac{1}{4}(1 - 0.31\alpha_V)$
$\bar{\psi}\gamma_5\gamma_\mu U_\mu\psi$	Z_A^{nI}	$\frac{1}{4}(1 + 0.91\alpha_V)$
$\bar{\psi}\gamma_\mu\psi$	Z_V^I	$\frac{1}{4}(1 - 0.82\alpha_V)$
$\bar{\psi}\gamma_\mu U_\mu\psi$	Z_V^{nI}	$\frac{1}{4}(1 - 1.00\alpha_V)$
$\bar{\psi}(1 + \gamma_\mu)U_\mu\psi + \dots$	Z_V^V	$\frac{1}{4}$

From the measured $\langle \frac{1}{3} \text{Tr} U_P \rangle$ [0.565 00(2) and 0.564 44(2)], we obtain $\alpha_V(3.41/a) = 0.1785$ and 0.1790 for $am_q = 0.01$ and 0.025 . These numbers are probably given with too much accuracy. With the coefficient of the $O(\alpha_V^2)$ correction in Eq. (4.7) assumed to be of order 1, this correction could easily change $\alpha_V(3.41/a)$ by 0.005 or so.

Lepage and Mackenzie give an $O(\alpha_s)$ tadpole-improved perturbative prediction for κ_c which works quite well for quenched simulations for $\beta > 5.7$:

$$\frac{1}{2\kappa_c} = 4 \langle \frac{1}{3} \text{Tr} U_P \rangle^{1/4} - 1.268 \alpha_V(1.03/a). \quad (4.8)$$

The coupling is measured at lower q since the UV-sensitive tadpoles have been removed. Using

$$\alpha_V(q)^{-1} = \beta_0 \ln \left[\frac{q}{\Lambda_V} \right]^2 + \frac{\beta_1}{\beta_0} \ln \left[\ln \left[\frac{q}{\Lambda_V} \right]^2 \right] \quad (4.9)$$

or

$$\Lambda_V/q = \left[\frac{1}{\beta_0 \alpha_V} \right]^{\beta_1/2\beta_0^2} \exp \left[-\frac{1}{2\beta_0 \alpha_V} \right], \quad (4.10)$$

where

$$\beta_0 = \frac{11 - \frac{2}{3}n_f}{4\pi} \quad (4.11)$$

and

$$\beta_1 = \frac{102 - \frac{38}{3}n_f}{16\pi^2} \quad (4.12)$$

are the first two coefficients of the β function, we run the α_V 's down to the lower scale. We then find the perturbative predictions of $\kappa_c = 0.1624$ and 0.1626 for $am_q = 0.01$ and 0.025 with $n_f = 2$, to be contrasted with the observed 0.1610 or 0.1613 . Taking into account our estimated uncertainty of $\alpha_V(3.41/a)$ of about 0.005 , which translates into an uncertainty in κ_c of about 0.001 , this is quite good agreement and is somewhat better than the prediction of 0.1636 which would obtain if $n_f = 0$.

The perturbative formulas are actually valid for massless quarks. Extrapolating $\langle \frac{1}{3} \text{Tr} U_P \rangle$ linearly in am_q to zero quark mass, we then obtain $\alpha_V(3.41/a) = 0.1782$ and $\kappa_c = 0.1623$. Given the uncertainty of about 0.001 in this quantity, it is again in quite good agreement with our extrapolated (again linearly in am_q) $\kappa_c(am_q = 0) = 0.1608(1)$. Along the way we find that $a\Lambda_V = 0.201$ or with a nominal lattice spacing $1/a \simeq 2.0(2)$ GeV from our spectroscopy and the conversion of [17]

$$\frac{\Lambda_{\overline{\text{MS}}}}{\Lambda_V} = \exp \left\{ -\frac{31N - 10n_f}{66N - 12n_f} \right\} \quad (4.13)$$

for an $\text{SU}(N)$ gauge group with n_f flavors of fermions that $\Lambda_{\overline{\text{MS}}} = 264(26)$ MeV, where $\overline{\text{MS}}$ denotes the modified minimal subtraction scheme. This is a lattice prediction which includes the effects of two light fermions. The error here comes only from the uncertainty in a^{-1} . The uncertainty in $\alpha_V(3.41/a)$ translates into an uncertainty

of about 20 MeV in $\Lambda_{\overline{\text{MS}}}$.

We now begin a series of specific calculations of matrix elements. When we speak of “conventional” calculations we mean that we use $\sqrt{2\kappa}$ field normalizations and do not remove tadpole terms from the perturbative Z factors; however, we use α_V for all coupling constants, but evaluated at a UV-dominated scale $\alpha_V(3.41/a) = 0.18$. For the tadpole-improved calculations, the coupling should be taken at a lower scale. Lepage and Mackenzie have not analyzed the optimal scale for each operator. However, it seems reasonable to take a scale similar to the one used for the tadpole-improved perturbative estimation of κ_c , $\alpha_V(1.03/a) = 0.31$. Since the perturbative predictions for κ_c are somewhat off, one might alternatively estimate this coupling from Eq. (4.7) using the measured values for both plaquette and κ_c . Using the values extrapolated to zero mass for these quantities, we obtain $\alpha_V(1.03/a) = 0.28$. We see that there is about a 10% uncertainty in the coupling constant needed for the perturbative Z factors, which implies an uncertainty of up to about 5% in the Z factors. In the following we will use for the tadpole-improved analysis a coupling $\alpha_V = 0.3$.

V. VECTOR MATRIX ELEMENTS

We have measured matrix elements of three vector current operators, the “local” vector current

$$V_\mu^l = \bar{\psi} \gamma_\mu \psi, \quad (5.1)$$

the “nonlocal” current

$$V_\mu^{\text{nl}} = \frac{1}{2} (\bar{\psi} \gamma_\mu U_\mu \psi + \text{H.c.}), \quad (5.2)$$

and the conserved Wilson current

$$V_\mu^W = \frac{1}{2} \{ \bar{\psi} [U_\mu (\gamma_\mu - 1) + U_\mu^\dagger (\gamma_\mu + 1)] \psi \}. \quad (5.3)$$

We extract the current matrix element from correlated fits to the three parameters of two propagators with the appropriate operator as an interpolating field.

We choose to quote our vector current matrix elements through the dimensionless parameter f_V :

$$Z_V \langle V | V_\mu | 0 \rangle = \frac{1}{f_V} m_V^2 \epsilon_\mu. \quad (5.4)$$

In terms of this definition, the width of a vector state (whose quarks have a charge e_Q in units of the electron's charge) to decay into an $e^+ e^-$ pair is

$$\frac{1}{f_V^2} = \frac{3\Gamma(V \rightarrow e^+ e^-)}{4\pi \alpha^3 e_Q^2 m_V}. \quad (5.5)$$

This is the optimal definition for a lattice calculation since there is no dependence on the lattice spacing. The Wilson current is conserved, but the other currents are multiplicatively renormalized. The renormalization factors for all three currents are shown in Table I.

How do the ratios of the Z factors measured experimentally compare with the perturbative predictions? We measure these factors by doing a correlated fit to the Wilson current and to one of the nonconserved currents. This will extract the $(1 + A\alpha_V)$ part of Z . Our results are

TABLE II. Fits to the ratio of conserved vector current to the local vector current $R^{w,l}$ with Wilson valence fermions and $am_q=0.01$ staggered sea quarks. In this and following tables, numbers in the “kind” column for mesons refers to their quark content: 1–6 refer to hopping parameters 0.1320, 0.1410, 0.1525, 0.1565, 0.1585, and 0.1600.

Kind	κ_{ave}	D_{min}	D_{max}	Ratio	χ^2/N_{DF}	C.L.
1 1	0.1320	11	16	0.497(0)	295.200/9	0.000
2 1	0.1365	11	16	0.508(0)	215.100/9	0.000
2 2	0.1410	7	16	0.520(0)	7.260/17	0.950
3 1	0.1422	11	16	0.513(0)	323.800/9	0.000
3 2	0.1467	7	16	0.528(0)	7.104/17	0.955
3 3	0.1525	8	16	0.536(0)	8.347/15	0.820
4 1	0.1442	11	16	0.512(1)	244.200/9	0.000
4 2	0.1487	7	16	0.530(0)	9.789/17	0.833
4 3	0.1545	8	16	0.537(0)	10.900/15	0.619
4 4	0.1565	11	16	0.541(1)	4.034/9	0.776
5 1	0.1452	11	16	0.513(1)	140.600/9	0.000
5 2	0.1497	8	16	0.531(1)	9.121/15	0.764
5 3	0.1555	11	16	0.539(1)	3.763/9	0.807
5 4	0.1575	11	16	0.542(1)	5.092/9	0.649
5 5	0.1585	11	16	0.543(2)	8.372/9	0.301
6 1	0.1460	11	16	0.516(2)	49.620/9	0.000
6 2	0.1505	8	16	0.531(1)	6.757/15	0.914
6 3	0.1562	10	16	0.538(1)	5.530/11	0.786
6 4	0.1583	11	16	0.542(2)	6.318/9	0.503
6 5	0.1593	11	16	0.543(4)	15.170/9	0.034
6 6	0.1600	8	16	0.539(5)	29.670/15	0.005

shown in Fig. 9 and Tables II–V. We find first that the Z factors show only a few percent variation with κ , justifying the contention that the κ dependence factorizes. However, the perturbative formula predicts a ratio of

$$R^{l,w} = \frac{\langle 0|J^w|V \rangle}{\langle 0|J^l|V \rangle} = Z^l/Z^w = 0.86$$

and

$$R^{\text{nl},w} = \frac{\langle 0|J^w|V \rangle}{\langle 0|J^{\text{nl}}|V \rangle} = Z^{\text{nl}}/Z^w = 0.83,$$

quite a bit larger than our data. Our data resemble old results from quenched simulations. For example, Maiani

TABLE III. Fits to the ratio of conserved vector current to the nonlocal vector current $R^{w,l}$ with Wilson valence fermions and $am_q=0.01$ staggered sea quarks.

Kind	κ_{ave}	D_{min}	D_{max}	Ratio	χ^2/N_{DF}	C.L.
1 1	0.1320	11	16	0.669(0)	282.200/7	0.000
2 1	0.1365	5	16	0.667(0)	229.400/19	0.000
2 2	0.1410	8	16	0.670(0)	16.090/13	0.244
3 1	0.1422	11	16	0.661(0)	282.100/7	0.000
3 2	0.1467	11	16	0.664(0)	6.271/7	0.508
3 3	0.1525	11	16	0.659(0)	5.092/7	0.649
4 1	0.1442	5	16	0.657(0)	247.900/19	0.000
4 2	0.1487	11	16	0.661(0)	4.352/7	0.738
4 3	0.1545	10	16	0.656(1)	8.247/9	0.509
4 4	0.1565	10	16	0.653(1)	8.357/9	0.499
5 1	0.1452	9	16	0.656(1)	141.300/11	0.000
5 2	0.1497	11	16	0.659(1)	4.703/7	0.696
5 3	0.1555	10	16	0.654(1)	10.380/9	0.321
5 4	0.1575	10	16	0.651(1)	9.104/9	0.428
5 5	0.1585	10	16	0.649(2)	8.220/9	0.512
6 1	0.1460	10	16	0.657(1)	51.500/9	0.000
6 2	0.1505	11	16	0.658(1)	5.426/7	0.608
6 3	0.1562	10	16	0.652(1)	11.180/9	0.264
6 4	0.1583	10	16	0.650(2)	7.584/9	0.577
6 5	0.1593	8	16	0.646(2)	12.850/13	0.459
6 6	0.1600	6	16	0.640(2)	17.690/17	0.409

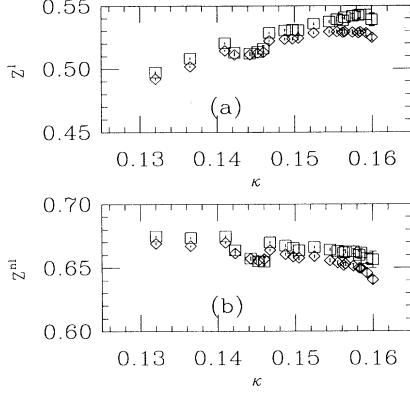


FIG. 9. Ratios of renormalization factors for (a) local and (b) nonlocal vector currents to the conserved current. Results from simulations with sea quark mass $am_q=0.01$ are shown as squares and for sea quark mass $am_q=0.025$ as diamonds.

and Martinelli [18] measured $R^{l,w}=0.57(2)$ and $R^{nl,w}=0.69(2)$ for these ratios in quenched $\beta=6.0$ simulations.

Results for the conserved current without any Z factors are shown in Tables VI and VII. Generically, all fits to mesons containing at least one of the heaviest quarks have low confidence levels.

Next, we wish to compare the measured f_V to experiment. We first choose to use the conserved Wilson current in this comparison. Our results are shown as a function of the dimensionless mass ratio m_P^2/m_V^2 in Fig. 1. The data undershoot the lightest vector mesons by about 25%, but appear to reproduce the experiment for

the $\psi(3100)$. Some of these shifts are known to be due to the use of “unimproved” operators. A calculation [13] at $\beta=6.0$ shows that a conserved and improved (CI) vector current would have a matrix element ratio $=\langle 0|J^{CL}|V\rangle/\langle 0|J^w|V\rangle=1.20$. It also finds $R^{l,w}=0.62$.

To compare with other simulations, we use a conventional normalization for our data. We show in Fig. 2 the conserved vector current and the local vector current. We rescale the latter by the Maiani-Martinelli factor of 0.57. Quenched $\beta=6.0$ results from Daniels *et al.* [19] and from the APE Collaboration [3] also use local currents and the same Z factor and are also shown. (If we assumed Z_V could be written as $1+A\alpha_s$ and just rescaled by the naive ratio of couplings $5.6/6.0$, it would change to 0.54, an invisible variation on the plot.) Our data are quite similar to the quenched results. Again, dependence of the matrix element on the sea quark mass is small.

Figures 1 and 2 show that the same lattice data can give quite different results depending on how it is converted to continuum numbers, even though the calculated quantity is dimensionless. For the vector operators, the discrepancy is largest for small quark mass.

VI. QUARK MASSES

The basic relation which gives us a quark mass is a continuum current algebra relation

$$\nabla_\mu \langle \bar{\psi}\gamma_5\psi(0)\bar{\psi}\gamma_5\gamma_\mu\psi(x) \rangle = 2m_q \langle \bar{\psi}\gamma_5\psi(0)\bar{\psi}\gamma_5\psi(x) \rangle. \quad (6.1)$$

If we convert to lattice operators, sum over spatial slices, and measure distance in the t direction, this becomes

TABLE IV. Fits to the ratio of conserved vector current to the local vector current $R^{w,l}$ with Wilson valence fermions and $am_q=0.025$ staggered sea quarks.

Kind	κ_{ave}	D_{min}	D_{max}	Ratio	χ^2/N_{DF}	C.L.
1 1	0.1320	11	16	0.492(0)	303.400/7	0.000
2 1	0.1365	5	16	0.520(0)	256.200/9	0.000
2 2	0.1410	10	16	0.514(0)	10.800/9	0.290
3 2	0.1422	11	16	0.511(0)	307.300/7	0.000
3.2	0.1467	11	16	0.522(0)	7.956/7	0.336
3 3	0.1525	11	16	0.528(0)	5.405/7	0.611
4 1	0.1442	6	16	0.511(0)	284.000/17	0.000
4 2	0.1487	11	16	0.523(0)	5.208/7	0.635
4 3	0.1545	11	16	0.529(1)	6.305/7	0.505
4 4	0.1565	10	16	0.529(1)	11.800/9	0.225
5 1	0.1452	6	16	0.512(0)	148.900/17	0.000
5 2	0.1497	11	16	0.524(1)	4.609/7	0.708
5 3	0.1555	11	16	0.529(1)	9.405/7	0.225
5 4	0.1575	10	16	0.529(1)	12.510/9	0.186
5 5	0.1585	8	16	0.529(1)	16.940/13	0.202
6 1	0.1460	6	16	0.513(1)	60.600/17	0.000
6 2	0.1505	11	16	0.524(1)	4.699/7	0.697
6 3	0.1562	11	16	0.529(1)	9.622/7	0.211
6 4	0.1583	8	16	0.528(1)	16.280/13	0.234
6 5	0.1593	8	16	0.528(2)	13.450/13	0.414
6 6	0.1600	6	16	0.525(2)	19.310/17	0.311

TABLE V. Fits to the ratio of conserved vector current vector current $R^{w,l}$ with Wilson valence fermions and $am_q=0.025$ staggered sea quarks.

Kind	κ_{ave}	D_{min}	D_{max}	Ratio	χ^2/N_{DF}	C.L.
1 1	0.1320	11	16	0.675(0)	273.400/9	0.000
2 1	0.1365	11	16	0.673(0)	193.900/9	0.000
2 2	0.1410	7	16	0.675(0)	8.975/17	0.879
3 1	0.1422	11	16	0.664(0)	302.400/9	0.000
3 2	0.1467	7	16	0.670(0)	6.298/17	0.974
3 3	0.1525	8	16	0.666(0)	8.032/15	0.842
4 1	0.1442	11	16	0.657(1)	233.300/9	0.000
4 2	0.1487	7	16	0.667(0)	8.239/17	0.914
4 3	0.1545	8	16	0.664(0)	10.480/15	0.654
4 4	0.1565	8	16	0.663(1)	15.910/5	0.254
5 1	0.1452	11	16	0.655(1)	140.100/9	0.000
5 2	0.1497	8	16	0.665(1)	7.415/15	0.880
5 3	0.1555	8	16	0.663(1)	13.730/15	0.393
5 4	0.1575	11	16	0.663(2)	8.265/9	0.310
5 5	0.1585	11	16	0.662(2)	11.480/9	0.119
6 1	0.1460	11	16	0.655(3)	47.740/9	0.000
6 2	0.1505	8	16	0.664(1)	5.736/15	0.955
6 3	0.1562	8	16	0.662(1)	11.280/15	0.587
6 4	0.1583	10	16	0.660(3)	11.440/11	0.247
6 5	0.1593	8	16	0.657(3)	28.220/15	0.008
6 6	0.1600	8	16	0.656(6)	31.820/15	0.003

$$Z_A \frac{\partial}{\partial t} \sum_{x,y,z} \langle \bar{\psi} \gamma_5 \psi(0) \bar{\psi} \gamma_5 \gamma_0 \psi(x) \rangle$$

$$= 2am_q Z_P \sum_{x,y,z} \langle \bar{\psi} \gamma_5 \psi(0) \bar{\psi} \gamma_5 \psi(x) \rangle. \quad (6.2)$$

There are many possibilities for defining an axial-vector current and for defining the derivative operator [18,20]. The most stable one we have found [21] is to say that,

$$\text{since } A(z) \approx \sinh[m_\pi(t - N_t/2)],$$

$$\frac{\partial A(t)}{\partial t} = m_\pi \cosh[m_\pi(t - N_t/2)]. \quad (6.3)$$

Then we extract the quark mass by fitting

$$P(t) = Z \{ \exp(-m_\pi t) + \exp[-m_\pi(N_t - t)] \} \quad (6.4)$$

TABLE VI. Fits to f_V for the conserved current with Wilson valence fermions and $am_q=0.01$ staggered sea quarks.

Kind	κ_{ave}	D_{min}	D_{max}	f_V	χ^2/N_{DF}	C.L.
1 1	0.1320	11	16	0.328(3)	180.100/7	0.000
2 1	0.1365	11	16	0.358(3)	117.900/7	0.000
2 2	0.1410	7	16	0.382(3)	13.930/15	0.672
3 1	0.1422	11	16	0.395(5)	198.900/7	0.000
3 2	0.1467	7	16	0.441(3)	8.662/15	0.950
3 3	0.1525	7	16	0.586(4)	12.960/15	0.739
4 1	0.1442	11	16	0.385(6)	162.100/7	0.000
4 2	0.1487	7	16	0.441(3)	7.704/15	0.972
4 3	0.1545	8	16	0.619(7)	7.502/13	0.942
4 4	0.1565	8	16	0.693(8)	9.074/13	0.874
5 1	0.1452	11	16	0.363(7)	95.980/7	0.000
5 2	0.1497	7	16	0.429(4)	8.382/15	0.958
5 3	0.1555	8	16	0.626(7)	8.065/13	0.921
5 4	0.1575	8	16	0.719(9)	11.320/13	0.730
5 5	0.1585	8	16	0.759(10)	14.450/13	0.492
6 1	0.1460	7	16	0.320(4)	50.520/15	0.000
6 2	0.1505	7	16	0.413(5)	10.290/15	0.891
6 3	0.1562	8	16	0.615(9)	8.379/13	0.908
6 4	0.1583	8	16	0.723(11)	14.060/13	0.521
6 5	0.1593	8	16	0.774(13)	20.420/13	0.156
6 6	0.1600	8	16	0.795(17)	27.450/13	0.025

TABLE VII. Fits to f_V for the conserved vector current with Wilson valence fermions and $am_q=0.025$ staggered sea quarks.

Kind	κ_{ave}	D_{min}	D_{max}	f_V	χ^2/N_{DF}	C.L.
1 1	0.1320	11	16	0.316(3)	160.400/7	0.000
2 1	0.1365	11	16	0.343(3)	110.300/7	0.000
2 2	0.1410	10	16	0.372(3)	9.104/9	0.612
3 1	0.1422	11	16	0.370(4)	147.800/7	0.000
3 2	0.1467	11	16	0.421(5)	6.977/7	0.640
3 3	0.1525	11	16	0.547(8)	9.368/7	0.404
4 1	0.1442	11	16	0.357(5)	101.400/7	0.000
4 2	0.1487	11	16	0.421(6)	6.547/7	0.684
4 3	0.1545	11	16	0.586(10)	11.230/7	0.260
4 4	0.1565	11	16	0.651(14)	14.560/7	0.104
5 1	0.1452	11	16	0.339(6)	62.480/7	0.000
5 2	0.1497	11	16	0.411(7)	8.366/7	0.498
5 3	0.1555	11	16	0.595(12)	15.330/7	0.082
5 4	0.1575	11	16	0.674(19)	16.550/7	0.056
5 5	0.1585	8	16	0.741(11)	26.590/13	0.032
6 1	0.1460	4	16	0.341(2)	51.810/21	0.001
6 2	0.1505	11	16	0.394(10)	12.590/7	0.182
6 3	0.1562	11	16	0.593(17)	16.650/7	0.054
6 4	0.1583	8	16	0.716(11)	24.740/13	0.054
6 5	0.1593	10	16	0.729(21)	11.660/9	0.390
6 6	0.1600	10	16	0.732(28)	8.907/9	0.630

and

$$A(t) = \frac{Z_P}{Z_A} \frac{2m_q}{m_\pi} Z \{ \exp(-m_\pi t) - \exp[-m_\pi(N_t - t)] \}. \quad (6.5)$$

We determine quark masses from both local and nonlocal axial-vector currents. Our results are shown in Tables VIII–XI. The reader should note that the best fits for mesons containing one or two of the heaviest quarks ($\kappa=0.1320$) are unacceptably poor. From the table readers can convince themselves that the average quark mass interpolates quite well among the different κ values—that is, $m_q(\kappa_1 + \kappa_2) \simeq \frac{1}{2}[m_q(\kappa_1) + m_q(\kappa_2)]$. As an alternate display, we show in Fig. 10 quark masses for all combinations of quarks as a function of $1/\kappa_{\text{ave}} - 1/\kappa_c$, where $1/\kappa_{\text{ave}} = 0.5(1/\kappa_1 + 1/\kappa_2)$. The data are remarkably linear.

We can compare our results to very simple theory. In the free-field limit, the relation between the quark mass and the hopping parameter for small quark mass is

$$am_q = \frac{1}{2} \left[\frac{1}{\kappa} - \frac{1}{\kappa_c} \right] \quad (6.6)$$

(with $\kappa_c = \frac{1}{8}$). From the discussion of Sec. III, we have

$$am_q = \ln \left[\frac{1 - 6\bar{\kappa}}{2\bar{\kappa}} \right], \quad (6.7)$$

with $\bar{\kappa} = \kappa/8\kappa_c$. We can take κ_c from our extrapolation of the pion mass and plot Eqs. (6.6) and (6.7) in Fig. 10. Both curves provide a good representation of the data. Note that this implies that the renormalization of the prefactor $\frac{1}{2}$ is much smaller than the renormalization of

κ_c , especially for the quark mass extracted from the local axial-vector current.

One should be able to measure κ_c from the point where the quark mass vanishes. This should serve as a reasonably independent check of the calculation of κ_c from the vanishing of the pion mass. (It is not completely independent, since the same lattices and some of the same operators are used in both extrapolations.) We previously reported $\kappa_c = 0.1610(1)$ for $am_q = 0.01$ and $am_q = 0.1613(1)$ for $am_q = 0.025$. The latter value was different from that found from simulations on 12^4 lattices, and it is important that it be rechecked. We do this

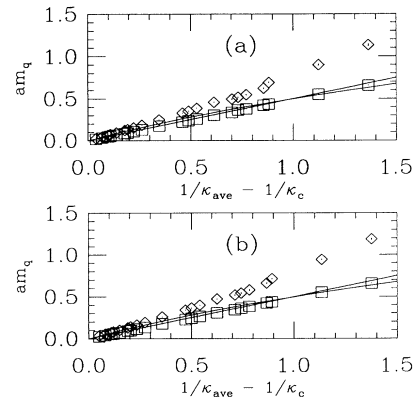


FIG. 10. Quark mass in lattice units as a function of $1/\kappa_{\text{ave}} - 1/\kappa_c$. Results for the local axial-vector current are shown as squares and for the nonlocal axial-vector current as diamonds. The lines show predictions of Eqs. (6.6) and (6.7). (a) Sea quark mass $am_q = 0.01$, (b) sea quark mass $am_q = 0.025$.

TABLE VIII. Fits to the quark mass from the local axial-vector current with Wilson valence fermions and $am_q = 0.01$ staggered sea quarks. All Z factors are set to unity.

Kind	κ_{ave}	D_{min}	D_{max}	am_q	χ^2/N_{DF}	C.L.
1 1	0.1320	11	16	0.4997(3)	309.300/7	0.000
2 1	0.1365	11	16	0.4186(3)	480.300/7	0.000
2 2	0.1410	8	16	0.3308(2)	6.212/13	0.859
3 1	0.1422	11	16	0.3204(3)	1037.000/7	0.000
3 2	0.1467	9	16	0.2300(2)	3.365/11	0.948
3 3	0.1525	9	16	0.1307(2)	7.943/11	0.540
4 1	0.1442	11	16	0.2870(4)	1016.000/7	0.000
4 2	0.1487	9	16	0.1963(2)	11.340/11	0.253
4 3	0.1545	9	16	0.0980(2)	10.400/11	0.319
4 4	0.1565	11	16	0.0656(3)	3.258/7	0.660
5 1	0.1452	11	16	0.2772(11)	985.600/7	0.000
5 2	0.1497	9	16	0.1800(2)	15.920/11	0.069
5 3	0.1555	11	16	0.0820(3)	2.810/7	0.729
5 4	0.1575	11	16	0.0502(3)	2.111/7	0.834
5 5	0.1585	11	16	0.0351(4)	1.361/7	0.929
6 1	0.1460	11	16	0.2545(7)	257.300/7	0.000
6 2	0.1505	9	16	0.1680(3)	12.320/11	0.196
6 3	0.1562	9	16	0.0708(3)	7.980/11	0.536
6 4	0.1583	11	16	0.0391(4)	1.445/7	0.919
6 5	0.1593	11	16	0.0242(4)	1.205/7	0.944
6 6	0.1600	8	16	0.0133(3)	6.659/13	0.826

as follows: We take only the six lightest (κ_1, κ_2) combinations (all combinations of the three lightest κ values). We take

$$am_q = A(1/\kappa - 1/\kappa_c) \quad (6.8)$$

as a model for the dependence of the quark mass on κ . All the data come from the same set of lattices and so are

strongly correlated. In order to assign an uncertainty to the fit parameters, we perform a jackknife fit, dropping 10 successive lattices from each of 10 subsets (containing 90 lattices) from the data, fitting each subset, extracting a κ_c , and averaging. We set all Z factors to unity; we are extrapolating the quark mass in lattice units with a lattice cutoff to zero. We report the results of these fits in Table

TABLE IX. Fits to the quark mass from the nonlocal axial-vector current with Wilson valence fermions and $am_q = 0.01$ staggered sea quarks. All Z factors are set to unity.

Kind	κ_{ave}	D_{min}	D_{max}	am_q	χ^2/N_{DF}	C.L.
1 1	0.1320	10	16	0.6153(54)	185.200/9	0.000
2 1	0.1365	10	16	0.4879(37)	200.800/9	0.000
2 2	0.1410	8	16	0.3753(21)	15.270/13	0.170
3 1	0.1422	11	16	0.3382(24)	483.400/7	0.000
3 2	0.1467	8	16	0.2480(11)	12.100/13	0.356
3 3	0.1525	7	16	0.1345(4)	22.330/15	0.050
4 1	0.1442	11	16	0.2965(20)	412.500/7	0.000
4 2	0.1487	7	16	0.2088(8)	13.290/15	0.426
4 3	0.1545	7	16	0.0997(3)	21.590/15	0.062
4 4	0.1565	7	16	0.0665(3)	23.060/15	0.041
5 1	0.1452	11	16	0.2800(21)	295.500/7	0.000
5 2	0.1497	7	16	0.1900(7)	14.750/15	0.323
5 3	0.1555	7	16	0.0833(3)	21.360/15	0.066
5 4	0.1575	11	16	0.0509(3)	7.486/7	0.187
5 5	0.1585	7	16	0.0356(3)	21.070/15	0.072
6 1	0.1460	11	16	0.2678(29)	135.300/7	0.000
6 2	0.1505	10	16	0.1774(12)	5.410/9	0.610
6 3	0.1562	7	16	0.0715(3)	20.130/15	0.092
6 4	0.1583	9	16	0.0399(3)	13.690/11	0.134
6 5	0.1593	7	16	0.0245(3)	17.200/15	0.190
6 6	0.1600	6	16	0.0132(3)	12.630/17	0.631

TABLE X. Fits to the quark mass from the local axial-vector current with Wilson valence fermions and $am_q=0.025$ staggered sea quarks. All Z factors are set to unity.

Kind	κ_{ave}	D_{min}	D_{max}	am_q	χ^2/N_{DF}	C.L.
1 1	0.1320	4	16	0.5005(2)	249.500/21	0.000
2 1	0.1365	11	16	0.4202(3)	365.600/7	0.000
2 2	0.1410	8	16	0.3333(2)	16.740/13	0.116
3 1	0.1422	11	16	0.3233(4)	792.400/7	0.000
3 2	0.1467	8	16	0.2328(2)	15.030/13	0.181
3 3	0.1525	8	16	0.1339(2)	25.070/13	0.009
4 1	0.1442	11	16	0.2910(4)	769.100/7	0.000
4 2	0.1487	8	16	0.1995(2)	17.890/13	0.084
4 3	0.1545	8	16	0.1016(2)	21.520/13	0.028
4 4	0.1565	8	16	0.0699(2)	17.080/13	0.106
5 1	0.1452	11	16	0.2741(5)	611.500/7	0.000
5 2	0.1497	7	16	0.1835(2)	24.890/15	0.024
5 3	0.1555	8	16	0.0860(2)	18.960/13	0.062
5 4	0.1575	8	16	0.0547(2)	14.820/13	0.191
5 5	0.1585	8	16	0.0398(2)	13.520/13	0.261
6 1	0.1460	11	16	0.2599(6)	381.600/7	0.000
6 2	0.1505	8	16	0.1718(3)	25.160/13	0.009
6 3	0.1562	8	16	0.0747(2)	17.310/13	0.099
6 4	0.1583	8	16	0.0437(2)	13.730/13	0.248
6 5	0.1593	7	16	0.0291(2)	16.060/15	0.246
6 6	0.1600	7	16	0.0184(3)	13.910/15	0.380

XII. The critical hopping parameter determined from the quark mass appears to be consistent with the value determined from the vanishing of the pion mass.

Finally, we can compare these Wilson quark masses to the quark masses of the staggered sea quarks. One way to do this is to match pion masses. The $am_q=0.025$ staggered pion has a mass in lattice units of about 0.42, and the $am_q=0.01$ staggered pion has a mass of about 0.26.

The former is about halfway between the masses of pseudoscalars with valence Wilson quarks of $\kappa=0.1565$ and 0.1585 , 0.47 and 0.36 (at sea quark mass $am_q=0.025$). The quark mass at those hopping parameters is 0.08 and 0.05. The $am_q=0.01$ pion lies between the $\kappa=0.1600$ and 0.1585 pions (0.21 and 0.33). However, the quark masses at those hopping parameters are 0.04–0.02. Thus the quark mass determined with the method of this sec-

TABLE XI. Fits to the quark mass from the nonlocal axial-vector current with Wilson valence fermions and $am_q=0.025$ staggered sea quarks. All Z factors are set to unity.

Kind	κ_{ave}	D_{min}	D_{max}	am_q	χ^2/N_{DF}	C.L.
1 1	0.1320	6	16	0.6457(44)	171.900/17	0.000
2 1	0.1365	6	16	0.5109(32)	189.200/17	0.000
2 2	0.1410	9	16	0.3872(26)	11.390/11	0.250
3 1	0.1422	11	16	0.3591(30)	362.600/7	0.000
3 2	0.1467	8	16	0.2560(13)	11.360/13	0.414
3 3	0.1525	9	16	0.1400(5)	20.970/11	0.013
4 1	0.1442	11	16	0.3148(25)	364.500/7	0.000
4 2	0.1487	7	16	0.2163(9)	13.000/15	0.448
4 3	0.1545	9	16	0.1046(4)	18.760/11	0.027
4 4	0.1565	9	16	0.0709(3)	13.150/11	0.156
5 1	0.1452	11	16	0.2941(24)	306.300/7	0.000
5 2	0.1497	7	16	0.1973(8)	12.790/15	0.464
5 3	0.1555	9	16	0.0880(3)	16.630/11	0.055
5 4	0.1575	9	16	0.0553(3)	10.260/11	0.330
5 5	0.1585	9	16	0.0401(3)	8.020/11	0.532
6 1	0.1460	9	16	0.2820(22)	195.000/11	0.000
6 2	0.1505	7	16	0.1837(8)	17.910/15	0.161
6 3	0.1562	8	16	0.0765(3)	18.200/13	0.077
6 4	0.1583	9	16	0.0442(3)	9.140/11	0.424
6 5	0.1593	9	16	0.0293(3)	7.500/11	0.585
6 6	0.1600	9	16	0.0184(3)	7.346/11	0.601

TABLE XII. Fits to κ_c from quark masses calculated from axial-vector current matrix elements, using pseudoscalar mesons with all combinations of light valence quarks.

Mass	Kind	κ_c	A
0.01	local	0.160 91(2)	0.431(2)
0.01	nonlocal	0.160 90(2)	0.528(4)
0.025	local	0.161 28(3)	0.422(2)
0.025	nonlocal	0.161 27(4)	0.518(4)

tion is much greater than the staggered quark mass at similar values of the pion mass.

VII. AXIAL-VECTOR MATRIX ELEMENTS

We measured matrix elements of two axial-vector current operators, the local current

$$A_0^{\text{loc}} = \bar{\psi} \gamma_0 \gamma_5 \psi \quad (7.1)$$

and the nonlocal operator

$$A_0^{\text{nl}} = \frac{1}{2} (\bar{\psi} U_0 \gamma_0 \gamma_5 \psi + \text{H.c.}) . \quad (7.2)$$

We used two source spinor combinations for the local operator: an interpolating field $\bar{\psi} \gamma_5 \psi$ and $\bar{\psi} \gamma_0 \gamma_5 \psi$. Only the first source was used with the nonlocal operator. This gives us a check of possible sensitivity to the source of our measurements. We quote answers in terms of the lattice pseudoscalar decay constant

$$Z_A \langle 0 | A_0 | P \rangle = f_P^L m_P . \quad (7.3)$$

Our values for f_P^L are given in Tables XIII and XIV and shown in Fig. 11 for local and nonlocal operators. The figure includes all Z factors from a tadpole-improved

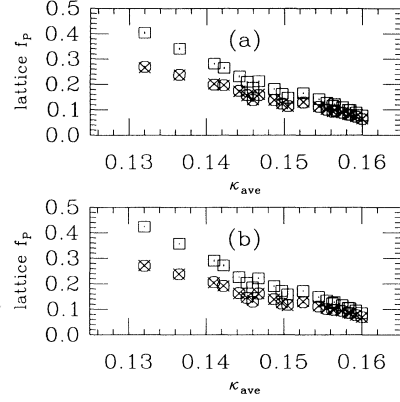


FIG. 11. Lattice f_P from axial-vector currents (including all Z factors from a tadpole-improved analysis) as a function of the average hopping parameter $1/2(\kappa_1 + \kappa_2)$. Data are labeled with crosses for the local current and a γ_5 source, octagons for the local current and a $\gamma_0 \gamma_5$ source, and squares for the nonlocal current. (a) $am_q = 0.01$, (b) $am_q = 0.025$.

calculation and lacks only a lattice spacing to show continuum numbers. The tables include no Z factors, to facilitate comparisons with other simulations (they are f_P^L/Z_A). Note from the figure that there is essentially no dependence on the source for the local operator.

We compare the ratio of Z factors from nonlocal axial-vector to local axial-vector currents. This ratio is shown in Fig. 12 and Tables XV and XVI. The expectation of perturbation theory is that this ratio is 1.23, independent of κ . The observed κ dependence is larger than for the vector currents, but still only about 20%.

TABLE XIII. Fits to pseudoscalar decay constant from local axial-vector currents, with Wilson valence fermions and $am_q = 0.01$ staggered sea quarks. All Z factors are set to unity.

Kind	κ_{ave}	D_{min}	D_{max}	f_P/Z_A	χ^2/N_{DF}	C.L.
1 1	0.1320	5	16	0.729(4)	95.440/19	0.000
2 1	0.1365	9	16	0.690(5)	51.340/11	0.000
2 2	0.1410	7	16	0.623(4)	8.756/15	0.890
3 1	0.1422	11	16	0.622(7)	80.430/7	0.000
3 2	0.1467	7	16	0.538(4)	5.709/15	0.984
3 3	0.1525	7	16	0.476(4)	7.733/15	0.934
4 1	0.1442	11	16	0.564(7)	74.330/7	0.000
4 2	0.1487	7	16	0.478(4)	6.101/15	0.978
4 3	0.1545	7	16	0.427(4)	9.271/15	0.863
4 4	0.1565	7	16	0.384(3)	11.060/15	0.748
5 1	0.1452	11	16	0.516(9)	60.020/7	0.000
5 2	0.1497	7	16	0.437(4)	7.849/15	0.930
5 3	0.1555	7	16	0.392(3)	9.891/15	0.827
5 4	0.1575	7	16	0.353(3)	11.060/15	0.748
5 5	0.1585	7	16	0.325(4)	10.950/15	0.756
6 1	0.1460	11	16	0.472(13)	39.700/7	0.000
6 2	0.1505	7	16	0.402(5)	13.560/15	0.559
6 3	0.1562	7	16	0.363(4)	12.100/15	0.671
6 4	0.1583	6	16	0.328(3)	12.090/17	0.795
6 5	0.1593	6	16	0.298(4)	11.330/17	0.839
6 6	0.1600	5	16	0.268(5)	17.670/19	0.545

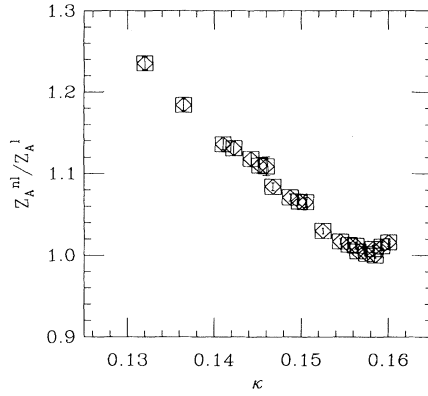


FIG. 12. Ratios of renormalization factors of nonlocal to local axial-vector currents. Results from simulations with sea quark mass $am_q=0.01$ are shown as squares and for sea quark mass $am_q=0.025$ as diamonds.

Our data are similar to the quenched $\beta=6$ results of Ref. [18], about 1.25 for the ratio. Note that the perturbative prediction and the operators themselves are not “improved.”

Next we wish to compare to experiment. There are two interesting quantities: f_π itself and the decay constants of heavy pseudoscalar mesons (such as the D meson). We calculate f_π by extrapolating our data for mesons made of degenerate quarks to κ_c , using the three lightest κ values. To present a number for f_D , we extrapolate light-quark-heavy-quark decay constants first to zero light quark mass; then we will interpolate in the heavy quark mass. The extrapolations are done using

jackknives. We do the extrapolations using both tadpole-improved and conventional renormalizations.

We find four values for f_π , corresponding to local and nonlocal operators with sea quark mass $am_q=0.01$ and 0.025 . In lattice units they are (with a tadpole-improved analysis) and, in order, local $am_q=0.01$, nonlocal $am_q=0.01$, local $am_q=0.025$, nonlocal $am_q=0.025$: $0.053(1)$, $0.074(1)$, $0.055(1)$, and $0.076(1)$. With a nominal lattice spacing of $1/a=2$ GeV, these numbers are $106(3)$, $148(3)$, $110(2)$, and $153(2)$ MeV. The numbers from a conventional analysis are $0.054(1)$, $0.089(2)$, $0.056(1)$, and $0.092(1)$ or $107(3)$, $179(3)$, $112(2)$, and $185(3)$ MeV. With our normalization, the experimental number is 132 MeV. The uncertainties are entirely from the extrapolation. The lattice spacing is uncertain to 10–15 %; this uncertainty dominates a final answer. We see little variation with sea quark mass; the variation with operator choice is much greater.

It has become customary to present heavy-light results as a graph of $f_P\sqrt{M_P}$ versus the inverse pseudoscalar mass $1/M_P$. To do this, we need a lattice spacing. We can use either some hadron mass or the measured f_π itself to set the scale. Using f_π divides out lattice-to-continuum renormalization factors (at zero quark mass). Note with the tadpole-improved field renormalization the factor $\sqrt{1-6\bar{\kappa}}$ or $2\kappa\exp(ma)$ is present in the field normalization. We carry out this extrapolation for each operator at each sea quark mass. The results of the extrapolations are shown in Tables XVII and XVIII and Figs. 3 and 4. The derived lattice spacings for the nonlocal operators (with conventional field normalization) are much larger than the nominal $1/a\simeq 2$ GeV from spectroscopy [2], while the lattice spacings for the conventionally normalized local operator and for the tadpole

TABLE XIV. Fits to pseudoscalar decay constant from local axial-vector currents, with Wilson valence fermions and $am_q=0.025$ staggered sea quarks. All Z factors are set to unity.

Kind	κ_{ave}	D_{min}	D_{max}	f_P/Z_A	χ^2/N_{DF}	C.L.
1 1	0.1320	10	16	0.743(7)	91.510/9	0.000
2 1	0.1365	10	16	0.692(6)	61.730/9	0.000
2 2	0.1410	11	16	0.624(6)	1.845/7	0.968
3 1	0.1422	10	16	0.603(6)	106.300/9	0.000
3 2	0.1467	11	16	0.538(6)	3.518/7	0.833
3 3	0.1525	11	16	0.475(6)	5.414/7	0.610
4 1	0.1442	7	16	0.530(5)	112.700/15	0.000
4 2	0.1487	11	16	0.480(6)	5.282/7	0.626
4 3	0.1545	11	16	0.428(7)	6.533/7	0.479
4 4	0.1565	8	16	0.399(4)	18.180/13	0.151
5 1	0.1452	8	16	0.488(5)	78.900/13	0.000
5 2	0.1497	11	16	0.442(7)	5.954/7	0.545
5 3	0.1555	11	16	0.396(7)	7.100/7	0.419
5 4	0.1575	8	16	0.370(4)	16.790/13	0.209
5 5	0.1585	8	16	0.341(4)	15.110/13	0.301
6 1	0.1460	8	16	0.456(6)	47.400/13	0.000
6 2	0.1505	11	16	0.407(9)	6.791/7	0.451
6 3	0.1562	8	16	0.384(4)	17.670/13	0.170
6 4	0.1583	8	16	0.344(4)	15.250/13	0.292
6 5	0.1593	8	16	0.315(4)	13.000/13	0.448
6 6	0.1600	8	16	0.284(5)	10.140/13	0.682

TABLE XV. Fits to ratio of local to nonlocal axial-vector currents, with Wilson valence fermions and $am_q = 0.01$ staggered sea quarks.

Kind	κ_{ave}	D_{min}	D_{max}	Ratio	χ^2/N_{DF}	C.L.
1 1	0.1320	7	16	1.235(8)	87.330/15	0.000
2 1	0.1365	7	16	1.184(7)	56.780/15	0.000
2 2	0.1410	8	16	1.136(6)	14.490/13	0.207
3 1	0.1422	11	16	1.131(9)	69.180/7	0.000
3 2	0.1467	7	16	1.084(4)	17.830/15	0.164
3 3	0.1525	7	16	1.030(3)	13.250/15	0.429
4 1	0.1442	11	16	1.118(9)	61.910/7	0.000
4 2	0.1487	7	16	1.071(4)	15.610/15	0.271
4 3	0.1545	7	16	1.017(3)	12.340/15	0.500
4 4	0.1565	7	16	1.005(2)	13.560/15	0.406
5 1	0.1452	11	16	1.110(9)	44.840/7	0.000
5 2	0.1497	7	16	1.066(4)	14.060/15	0.370
5 3	0.1555	7	16	1.013(3)	12.830/15	0.461
5 4	0.1575	7	16	1.002(3)	15.070/15	0.303
5 5	0.1585	7	16	1.000(3)	16.880/15	0.205
6 1	0.1460	10	16	1.109(11)	30.560/9	0.000
6 2	0.1505	7	16	1.065(5)	13.920/15	0.380
6 3	0.1562	7	16	1.012(4)	15.050/15	0.304
6 4	0.1583	10	16	1.008(4)	6.295/9	0.506
6 5	0.1593	10	16	1.011(5)	7.229/9	0.405
6 6	0.1600	6	16	1.016(4)	19.990/17	0.172

operators are much closer to this number. This is a reflection of the large f_π results for this operator and normalization choice reported above. In the figures we show other recent calculations [5,22–24] of heavy-light decay constants which as far as we can tell were analyzed similarly to our tadpole-improved or conventional approaches. It is clear from the figures that our data is rather similar to the results of quenched simulations,

when the analyses are performed in the same way. It is also clear that the choice of field normalization has a drastic effect on the final answer. Note from Tables XIII and XIV that while we have carried out extrapolations for mesons containing a $\kappa=0.1320$ quark, the fits of these quantities before extrapolation have unacceptably poor confidence levels.

Now we attempt to predict f_D . We fit various com-

TABLE XVI. Fits to ratio of local to nonlocal axial-vector currents, with Wilson valence fermions and $am_q = 0.025$ staggered sea quarks.

Kind	κ_{ave}	D_{min}	D_{max}	Ratio	χ^2/N_{DF}	C.L.
1 1	0.1320	6	16	1.291(9)	91.110/17	0.000
2 1	0.1365	4	16	1.211(5)	67.170/21	0.000
2 2	0.1410	9	16	1.162(8)	10.670/11	0.299
3 1	0.1422	11	16	1.149(9)	69.450/7	0.000
3 2	0.1467	8	16	1.098(5)	16.010/13	0.141
3 3	0.1525	7	16	1.044(3)	18.140/15	0.152
4 1	0.1442	11	16	1.128(8)	62.960/7	0.000
4 2	0.1487	7	16	1.085(4)	20.200/15	0.090
4 3	0.1545	7	16	1.030(2)	16.240/15	0.236
4 4	0.1565	7	16	1.017(2)	13.140/15	0.437
5 1	0.1452	7	16	1.133(6)	67.940/15	0.000
5 2	0.1497	7	16	1.079(4)	20.050/15	0.094
5 3	0.1555	7	16	1.025(2)	14.480/15	0.341
5 4	0.1575	7	16	1.013(2)	11.300/15	0.586
5 5	0.1585	7	16	1.009(2)	9.734/15	0.716
6 1	0.1460	4	16	1.133(4)	50.410/21	0.000
6 2	0.1505	7	16	1.075(4)	20.680/15	0.080
6 3	0.1562	7	16	1.023(2)	12.970/15	0.450
6 4	0.1583	7	16	1.011(2)	9.669/15	0.721
6 5	0.1593	7	16	1.009(2)	8.447/15	0.813
6 6	0.1600	4	16	1.013(2)	19.330/21	0.436

TABLE XVII. Lattice spacing and table of masses and $f_P\sqrt{M_P}$ from axial-vector current matrix elements, from jack-knife extrapolations to zero light quark mass, using tadpole-improved perturbation theory.

am_q	Kind	$1/a$ (GeV)	Mass (GeV)	$f_P\sqrt{m_P}$ (GeV ^{3/2})
0.01	local	2.51	2.42	0.509(18)
			1.84	0.349(8)
			1.12	0.225(3)
			0.81	0.166(2)
	nonlocal	1.80	1.72	0.449(1)
			1.32	0.314(4)
			0.80	0.182(2)
			0.58	0.141(2)
0.025	local	2.41	2.31	0.458(22)
			1.79	0.334(12)
			1.11	0.221(7)
			0.83	0.168(4)
	nonlocal	1.74	1.65	0.417(7)
			1.30	0.319(7)
			0.81	0.198(2)
			0.60	0.145(2)

binations of our data points to the form

$$f_P\sqrt{M_P} = A + \frac{B}{M_P} \quad (7.4)$$

or

$$f_P\sqrt{M_P} = A + \frac{B}{M_P} + \frac{B}{M_P^2} \quad (7.5)$$

We discard the heaviest mass points since their confidence level is poor. A linear extrapolation represents the data poorly. (None of our heavy quarks are really heavy.) Quadratic interpolations through all the matrix elements of local operators or of all the nonlo-

TABLE XVIII. Lattice spacing and table of masses and $f_P\sqrt{M_P}$ from axial-vector current matrix elements, from jack-knife extrapolations to zero light quark mass, using conventional Z factors.

am_q	Kind	$1/a$ (GeV)	Mass (GeV)	$f_P\sqrt{m_P}$ (GeV ^{3/2})
0.01	local	2.48	2.39	0.361(12)
			1.81	0.271(6)
			1.10	0.196(2)
			0.80	0.153(1)
	nonlocal	1.49	1.42	0.292(8)
			1.09	0.224(2)
			0.66	0.155(2)
			0.48	0.118(2)
0.025	local	2.38	2.28	0.326(16)
			1.76	0.260(9)
			1.09	0.195(6)
			0.81	0.154(3)
	nonlocal	1.43	1.34	0.266(16)
			1.03	0.219(2)
			0.65	0.156(1)
			0.48	0.119(1)

cal operators (of both sea quark masses) are shown in Figs. 3 and 4 (with recent data from Refs. [22–24,5]). The data of Ref. [5] are converted from their figure to a measurement of $f_P\sqrt{M_P}$ by us [25]. The conventional analysis undershoots and the tadpole-improved analysis overshoots the static quark data of Refs. [26,27], which were not included in the fits.

With the fit, we can then interpolate to the D and B meson mass. With a tadpole-improved analysis find $f_D=256(5)$ MeV and $f_B=232(9)$ MeV from the local axial-vector current, and $f_D=287(4)$ MeV and $f_B=235(5)$ MeV from the nonlocal axial-vector current. The uncertainty is completely in the extrapolation. Interpolating the conventionally normalized lattice data gives $f_D=200(4)$ MeV and $f_B=160(7)$ MeV from the local axial-vector current and $f_D=208(4)$ MeV and $f_B=152(4)$ MeV from the nonlocal axial-vector current. We think it is reasonable to include a 10% overall uncertainty just from the lattice spacing in addition to a systematic uncertainty from the choice of operator. This is about a 20 MeV plus 10–20 MeV effect. The uncertainty due to the choice of α_s is quite small since it tends to cancel in taking a ratio to f_π ; for example, in the local axial-vector current with conventional normalization the variation is 4 MeV when α_s changes from 0.17 to 0.18.

Note that the tadpole-improved data also overshoot the data of Ref. [5]. These data are from a lattice coupling $\beta=6.3$ or a lattice spacing $1/a=3.2$ GeV as compared to our $1/a \simeq 2$ GeV. Thus the values of the D meson masses (in lattice units) differ by about 30%. More importantly, in our simulations the D meson has a mass in lattice units of about 0.93, which is very heavy. Only for the lighter masses do our data and that of Ref. [5] agree; only for lighter masses do the pseudoscalar masses become small compared to an inverse lattice spacing.

Recent lattice predictions for f_D (see [5,23,22,28]) lie near about 200 MeV. Without more theoretical input we do not know whether the difference in our predictions with tadpole improvement or with the conventional normalization is due to a large lattice spacing, represents a lattice-to-continuum systematic which should be included in the overall uncertainty of the lattice prediction, or whether one method of analysis is to be favored over the other for theoretical reasons. Certainly, the effects of sea quarks are small compared to other uncertainties.

Finally, we can obtain f_{D_s} . The number has recently been determined by experiment [29] to be $232 \pm 45 \pm 20 \pm 48$ MeV, and so the tadpole-improved numbers are already in conflict with experiment. We use the $\kappa=0.1585$ quark as the strange quark, since the mass of its vector meson is about 1 GeV (the ϕ mass) with an inverse lattice spacing of 2 GeV [2]. Using the conventional normalization and a lattice spacing determined by f_π , we find $f_{D_s}=220$ MeV from the local operator at either sea quark mass. We estimate the uncertainty on this number to be at least 20 MeV from the lattice spacing and 5 MeV in the intrinsic uncertainty of the lattice measurement. Decay constants measured with tadpole improvement are much larger (as they are for f_D): For ex-

ample, the local operator would give 298 or 264 MeV at $am_q = 0.01$ or 0.025 ; both nonlocal axial-vector current operators are also quite large, about 320 MeV. This is in conflict with experiment. Again, we remind the reader that the masses of these states are about 1.0 (in lattice units). This is uncomfortably large.

VIII. CONCLUSIONS

The data we have presented look rather similar to quenched simulations at a lattice spacing of $1/a \simeq 2$ GeV. The effects of different mass sea quarks are small. We see few percent effects on the vector decay constant, but any effects of sea quarks in the axial-vector current matrix elements are masked by uncertainties in the lattice spacing and systematic differences in the local and nonlocal operators. The one place we see definite influence of sea quarks is in the semiperturbative calculation of κ_c . There, a better prediction of κ_c needs a coupling constant which evolves under the influence of two dynamical flavors of quarks. But for experimental observables the effects of dynamical fermions seem to be subsumed into renormalizations of lattice parameters. The biggest uncertainties in these calculations, in fact, do not seem to be the lattice

numbers, but the conversion of lattice numbers into continuum numbers. The only way a pure numerical simulation can reduce those systematics is by reducing the lattice spacing to such a point that the coupling constant is small, independent of whether or not sea quarks are present.

ACKNOWLEDGMENTS

This work was supported by the U.S. Department of Energy under Contracts Nos. DE-FG02-85ER-40213, DE-FG02-91ER-40672, DE-AC02-84ER-40125, and W-31-109-ENG-38, and by the National Science Foundation under Grants Nos. NSF-PHY87-01775, NSF-PHY89-04035, and NSF-PHY86-14185. The computations were carried out at the Florida State University Supercomputer Computations Research Institute which is partially funded by the U.S. Department of Energy through Contract No. DE-FC05-85ER250000. We would like to thank P. Lepage and P. Mackenzie for discussions about Ref. [4], J. Fingberg for checking a calculation, and J. Labrenz and O. Pène for providing their data. We thank T. Kitchens and J. Mandula for their continuing support and encouragement.

-
- [1] K. Bitar *et al.*, Phys. Rev. Lett. **65**, 2106 (1990); Phys. Rev. D **42**, 3794 (1990).
 - [2] K. Bitar *et al.*, Phys. Rev. D **46**, 2169 (1992).
 - [3] S. Cabasino *et al.*, Phys. Lett. B **258**, 195 (1991). The data for f_V must be corrected by a factor of $\sqrt{\exp(-m_\rho)}$; and (private communication to R. Gupta).
 - [4] G. Peter Lepage and Paul B. Mackenzie, FERMILAB Report No. FERMILAB-PUB-91/355-T (unpublished).
 - [5] C. Bernard, C. Heard, J. Labrenz, and A. Soni, in *Lattice '91*, Proceedings of the International Symposium, Tsukuba, Japan, 1991, edited by M. Fukugita, Y. Iwasaki, M. Okawa, and A. Ukawa [Nucl. Phys. B (Proc. Suppl.) **26**, 384 (1992)]; C. Bernard, J. Labrenz, and A. Soni, in *Lattice '92*, Proceedings of the International Symposium, Amsterdam, 1992, edited by J. Smit and P. van Baal [*ibid.* **30**, 465 (1993)].
 - [6] H. C. Andersen, J. Chem. Phys. **72**, 2384 (1980); S. Duane, Nucl. Phys. **B257**, 652 (1985); S. Duane and J. Kogut, Phys. Rev. Lett. **55**, 2774 (1985); S. Gottlieb, W. Liu, D. Toussaint, R. Renkin, and R. Sugar, Phys. Rev. D **35**, 2531 (1987).
 - [7] J. E. Mandula and M. C. Ogilvie, Phys. Lett. B **248**, 156 (1990).
 - [8] T. DeGrand, Comput. Phys. Commun. **52**, 161 (1988).
 - [9] C. Liu, in *Lattice '90*, Proceedings of the International Symposium, Tallahassee, Florida, 1990, edited by U. M. Heller, A. D. Kennedy, and S. Sanielevici [Nucl. Phys. B (Proc. Suppl.) **20**, 149 (1991)]; A. D. Kennedy, Int. J. Mod. Phys. C **3**, 1 (1992).
 - [10] For a discussion of this fitting method, see D. Toussaint, in *From Actions to Answers*, Proceedings of the 1989 Theoretical Advanced Summer Institute on Particle Physics, Boulder, Colorado, edited by T. DeGrand and D. Toussaint (World Scientific, Singapore, 1990).
 - [11] Compare the discussion by S. Hashimoto and Y. Saeki, in *Lattice '91* [5], p. 381.
 - [12] K. Symanzik, Nucl. Phys. **B226**, 187 (1983).
 - [13] G. Martinelli, C. Sachrajda, and A. Vladikas, in *Lattice '90* [9], p. 448.
 - [14] R. Groot, J. Hoek, and J. Smit, Nucl. Phys. **B237**, 111 (1984).
 - [15] G. Martinelli and Y.-C. Zhang, Phys. Lett. **123B**, 433 (1983).
 - [16] This corrects for the omission of the n_f dependence in [4].
 - [17] This relation can be inferred from the definition of Λ_V in [4] and A. Billoire, Phys. Lett. **104B**, 472 (1981).
 - [18] L. Maiani and G. Martinelli, Phys. Lett. B **178**, 265 (1986).
 - [19] D. Daniel, R. Gupta, G. Kilcup, A. Patel, and S. Sharpe, Phys. Rev. D **46**, 3130 (1992); Report No. UW-PT-92-05 (unpublished).
 - [20] Y. Iwasaki, K. Kanaya, S. Sakai, and T. Yoshie, Phys. Rev. Lett. **69**, 21 (1992).
 - [21] C. Bernard *et al.*, Phys. Rev. D **46**, 4741 (1992).
 - [22] M. B. Gavela *et al.*, Phys. Lett. B **206**, 113 (1988).
 - [23] A. Abada *et al.*, in *Lattice '91* [5], p. 344.
 - [24] T. DeGrand and R. Loft, Phys. Rev. D **38**, 954 (1988).
 - [25] We would like to thank J. Labrenz for discussions about this data.
 - [26] C. Alexandrou *et al.*, Phys. Lett. B **256**, 60 (1991).
 - [27] C. Allton *et al.*, Nucl. Phys. **B349**, 598 (1991).
 - [28] D. G. Richards *et al.*, in *Lattice '92* [5], p. 389.
 - [29] S. Aoki *et al.*, CERN Report No. CERN-PPE/92-157, 1992 (unpublished).